

Air-Breathing Laminar Flow-Based Microfluidic Fuel Cell

Ranga S. Jayashree,[†] Lajos Gancs,[‡] Eric R. Choban,^{†,‡} Alex Primak,[§] Dilip Natarajan,[§] Larry J. Markoski,^{*,§} and Paul J. A. Kenis^{*,†,‡}

Department of Chemical & Biomolecular Engineering, and the Beckman Institute for Advanced Science and Technology, University of Illinois at Urbana-Champaign, 600 South Mathews Avenue, Urbana, Illinois 61801, and INI Power Systems, 136 Quade Drive, Cary, North Carolina 27513

Received July 11, 2005; E-mail: larry@inipower.com; kenis@uiuc.edu

This communication reports the design, assembly, and performance of an air-breathing laminar flow-based microfluidic fuel cell. Micro fuel cells have long been recognized as promising high energy density power sources for portable applications. Many advances in micro fuel cell development have been made, ranging from designs obtained by downscaling macroscale fuel cell technology¹ to novel designs that utilize the physical properties of the microscale, such as laminar flow^{2–4} as well as other microfabricated^{1,5} and microfluidic cells.⁶

Recent efforts have shown that the microfluidic transport phenomenon of laminar flow can be utilized to create the necessary compartmentalization of the fuel and oxidant streams in a single channel without the need of a physical barrier such as a membrane while still allowing ionic transport.^{2–4} In these multistream *laminar flow-based fuel cells* (LFFCs), an aqueous stream containing a liquid fuel, such as formic acid, methanol, or dissolved hydrogen, and an aqueous stream containing an oxidant, such as dissolved oxygen, permanganate, or hydrogen peroxide, are introduced into a single microfluidic channel in which the opposing sidewalls are the anode and cathode (Figure 1a). Several of the technical issues encountered in more conventional, Nafion membrane-based direct methanol fuel cells—*anode dry-out, cathode flooding, and fuel crossover*—can be avoided. Moreover, LFFCs are media flexible; the composition of the fuel and oxidant streams (e.g., pH) can be chosen independently, providing another way to improve reaction kinetics and open cell potentials.⁷

Moderate to high current densities from LFFCs can be obtained if highly soluble oxidants, such as vanadium-based redox couples² or permanganate,⁸ are used. Ideally the use of oxygen as the oxidant is preferred since it is readily available from the atmosphere for most envisioned fuel cell applications. To date, the performance of LFFCs using dissolved oxygen as the oxidant has been mass transfer limited at the cathode mainly due to low diffusivity (2×10^{-5} cm²/s).^{2,4} Also, the low oxygen concentration (2–4 mM) provides an insufficient driving force to replenish the depletion boundary layer on the cathode. This limitation can be addressed using fluids with higher oxygen concentration,⁸ or a more sophisticated microfluidic design with multiple inlets enabling boundary layer replenishment. Here, we address this cathode limitation by the integration of a porous air-exposed gas diffusion electrode (GDE) as the cathode into a laminar flow-based microfluidic fuel cell (Figure 1b) enabling oxygen delivery directly from air. GDEs are used, for example, in hydrogen fuel cells as the interface between the gaseous fuel/oxidant supply streams and the hydrated Nafion membrane, enabling efficient transport of the fuel and oxidant to the catalyst layers.⁹ A LFFC with a GDE as the cathode is expected to perform better than previous LFFCs in which dissolved oxygen is the oxidant source, as a result of the 4 orders

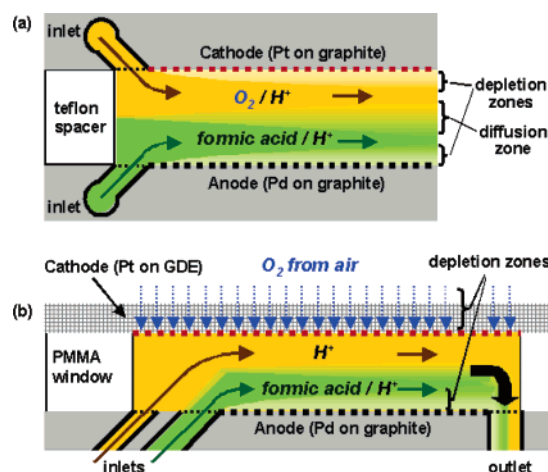


Figure 1. Schematic designs of (a) a LFFC with an oxygen-saturated stream as the oxidant supply^{2,4,7} and (b) a LFFC with a porous, air-breathing gas diffusion electrode (GDE) as the cathode. The rate of replenishment of oxygen from air (b) is much faster than from solution (a).

of magnitude higher diffusion coefficient of oxygen in air (0.2 cm²/s) than in aqueous media (2×10^{-5} cm²/s) as well as the higher concentration of oxygen in air (10 mM) than in aqueous media (2–4 mM). These differences all will enhance the oxygen reduction reaction rate (vide infra).

This new LFFC (Figure 1b) is comprised of a poly(methyl methacrylate) (PMMA) window to form the microfluidic channel, a graphite plate covered with Pd black nanoparticles as the anode, and Toray carbon paper GDE covered with Pt black nanoparticles as the cathode. A formic acid-containing 0.5 M sulfuric acid stream enters the cell through the second, wider inlet in the graphite sheet and flows over the GDE, while an electrolyte stream containing 0.5 M sulfuric acid only enters through the first inlet and prevents formic acid from reaching the GDE cathode. See Supporting Information for further details.

Polarization curves (Figure 2a) were obtained under ambient conditions using an in-house built test station (Supporting Information). For a formic acid concentration of 0.1 M, the potential drops sharply at a current density of about 20 mA/cm², which is characteristic of a mass transfer limited cell. At higher formic acid concentration, the polarization curves lack this shape, indicating that the mass transfer limitation has been eliminated. The best performance is observed for a formic acid concentration of 1 M: a maximum current density of about 130 mA/cm² and a maximum power density of 26 mW/cm² (Figure 2a and b). Both values are significantly higher than the best current and power densities reported for LFFCs operated with an oxygen-saturated aqueous stream (~ 14 mA/cm² and 5 mW/cm²).^{2,4,7} For comparison, the mass transfer limited performance of a LFFC without a GDE operated with 1 M formic acid as the fuel and dissolved oxygen in 0.5 M

[†] Department of Chemical & Biomolecular Engineering, University of Illinois.

[‡] Beckman Institute for Advanced Science and Technology, University of Illinois.

[§] INI Power Systems.

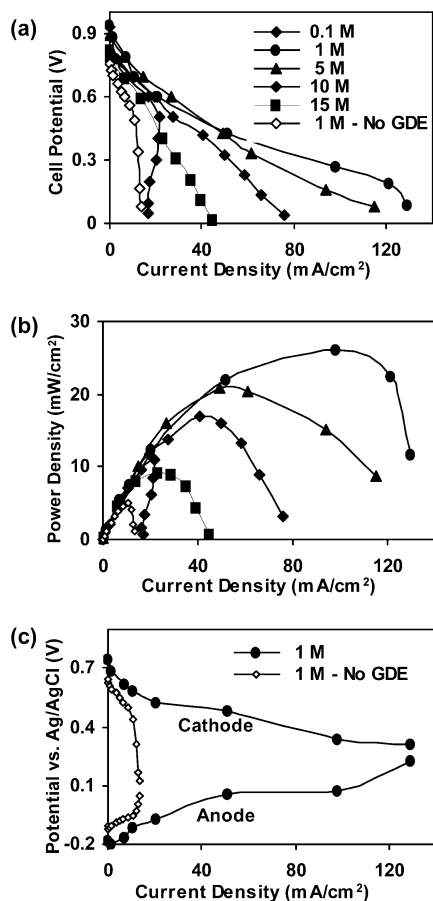


Figure 2. (a) Polarization and (b) power density curves, all at room temperature, for an air-breathing LFFC with a GDE as the cathode for different concentrations of formic acid as the fuel. (c) Anodic and cathodic potentials versus Ag/AgCl using 1 M HCOOH in 0.5 M H₂SO₄ as fuel stream. For comparison, data of a LFFC without a GDE operated with dissolved oxygen are plotted.⁸

sulfuric acid is shown in Figure 2a and b, as well. At [HCOOH] > 1 M, the performance gradually drops, which can be attributed to lowering of the conductivity of the anode stream at higher [HCOOH] and some diffusional crossover of formic acid to the cathodic stream.⁸ Fuel crossover, while not an issue for direct formic acid fuel cells (DFAFCs) with a Nafion membrane,^{1b} can be eliminated in LFFCs by balancing flow rates and cell dimensions, or by design changes that minimize the total area of the liquid–liquid interface.

Figure 2c shows the individual cathodic and anodic performance for the experiment with 1 M formic acid as the fuel, both for a LFFC with and without GDE.¹⁰ For the LFFC without a GDE, in which an oxygen-saturated sulfuric acid was used as the oxidant, a sharp drop in cathodic potential can be observed at 8–10 mA/cm² due to the slow rate of replenishment of oxygen in aqueous media. In contrast, the LFFC with a GDE exhibits a much smaller drop in cathodic potential while achieving current densities that are more than 10 times higher. The improved performance of the anode of the LFFC with GDE is due to optimized anode preparation (Supporting Information). These curves clearly show that introduction of a GDE mitigated the mass transfer limitations at the cathode.

The unoptimized utilization of formic acid for this LFFC with a GDE as the cathode, using a 1 M formic acid fuel stream, is about 8%, which is already significantly higher than the <1% fuel utilization of the LFFCs reported earlier.^{2,4,7} In subsequent experiments at lower flow rates (e.g., 0.1 mL/min), we achieved a single pass fuel utilization of 33%, however, at the expense of a drop in

power density to 10 mW/cm². In laminar flow-based fuel cells, the electrode-to-electrode distances, the electrode designs, and fuel concentrations can be adjusted appropriately to maximize performance and fuel utilization per single pass.^{2–4,7,8} Through simulation, Bazyk et al. have already shown that a fuel utilization as high as 52% can be obtained for certain designs in combination with certain operation conditions.¹¹ Further improvement of fuel utilization per pass can be accomplished by implementation of multiple inlets (or outlets) to replenish (remove) the depleted boundary layer on the anode side. To create a LFFC-based power source with acceptable energy conversion efficiency, multiple LFFCs have to be integrated in parallel (scaling out). Also, the fuel and electrolyte streams have to be split and recirculated with the fuel stream being replenished on the return path. To split the streams while avoiding extensive diffusional mixing, we use a separator plate¹² on which we will report in more detail shortly.

In sum, air-breathing laminar flow fuel cells with power densities as high as 26 mW/cm² were obtained through integration of a GDE as the cathode, which significantly enhanced the oxygen reduction reaction rate. A GDE cathode in these unconventional fuel cells addresses the mass transfer issues that to date limited the performance of LFFCs. Moreover, the need for oxygen-saturated oxidant streams or alternative highly soluble oxidants has been eliminated. Like with most active direct liquid fuel cell systems (e.g., DMFCs), electrolyte recirculation is required for LFFCs, which reduces the overall energy density of a fuel cell system. Compared to the volume of necessary pump, electronics, etc., the volume of recirculating fluids including the additional isolation stream used in a LFFC can be kept small, thus limiting the extent of this recirculation burden on a fuel cell system's specific energy. Further optimization of both single LFFC performance and integration of multiple LFFCs in a recirculating fuel cell system is the topic of our current research.

Acknowledgment. This work was supported through an STTR Phase II grant (Contract No. W911NF-04-C-0113) from ARO to INI Power Systems and the University of Illinois. The authors thank Seong Kee Yoon and Daniela Egas for helpful discussions.

Supporting Information Available: Detailed descriptions of cell assembly, operation, and characterization. This material is available free of charge via the Internet at <http://pubs.acs.org>.

References

- (1) (a) Kelley, S. C.; Deluga, G. A.; Smyrl, W. H. *Electrochem. Solid-State Lett.* **2000**, *3*, 407–409. (b) Rice, C.; Ha, S.; Masel, R. I.; Waszczuk, P.; Wieckowski, A.; Barnard, T. *J. Power Sources* **2002**, *111*, 83–89. (c) Meyers, J. P.; Maynard, H. L. *J. Power Sources* **2002**, *109*, 76–88. (d) Shimizu, T.; Momma, T.; Mohamedi, M.; Osaka, T.; Sarangapani, S. *J. Power Sources* **2004**, *137*, 277–283. (e) Li, J.; Moore, C.; Kohl, P. A. *J. Power Sources* **2004**, *138*, 211–215. (f) Gottesfeld, S. *Abstracts of Papers*; American Chemical Society: Washington, DC, 2004, 228, U653–U653.
- (2) (a) Choban, E. R.; Markoski, L. J.; Wieckowski, A.; Kenis, P. J. A. *J. Power Sources* **2004**, *128*, 54–60. (b) Markoski, L. J.; Moore, J. S.; Lyding, J. L. U.S. Patent 6,713,206, 2004.
- (3) Ferrigno, R.; Stroock, A. D.; Clark, T. D.; Mayer, M.; Whitesides, G. M. *J. Am. Chem. Soc.* **2002**, *124*, 12930–12931.
- (4) Cohen, J. L.; Westly, D. A.; Pechenik, A.; Abruna, H. D. *J. Power Sources* **2005**, *139*, 96–105.
- (5) Yeom, J.; Mozsai, G. Z.; Flachsbart, B. R.; Choban, E. R.; Asthana, A.; Shannon, M. A.; Kenis, P. J. A. *Sens. Actuators, B* **2005**, *107*, 882–891.
- (6) Mitrovski, S. M.; Elliott, L. C. C.; Nuzzo, R. G. *Langmuir* **2004**, *20*, 6974–6976.
- (7) (a) Choban, E. R.; Spendelow, J. S.; Gancs, L.; Wieckowski, A.; Kenis, P. J. A. *Electrochim. Acta* **2005**, *50*, 5390–5398. (b) Cohen, J. L.; Volpe, D. J.; Westly, D. A.; Pechenik, A.; Abruna, H. D. *Langmuir* **2005**, *21*, 3544–3550.
- (8) Choban, E. R.; Waszczuk, P.; Yoon, S.-K.; Gancs, L.; Jayashree, R. S.; Markoski, L. J.; Kenis, P. J. A. Manuscript in preparation.
- (9) Litster, S.; McLean, G. *J. Power Sources* **2004**, *130*, 61–76.
- (10) Choban, E. R.; Waszczuk, P.; Kenis, P. J. A. *Electrochem. Solid-State Lett.* **2005**, *8*, A348–A352.
- (11) Bazylak, A.; Sinton, D.; Djilali, N. *J. Power Sources* **2005**, *143*, 57–66.
- (12) Markoski, L. J.; Primak, A.; Kenis, P. J. A. 207th ECS Meeting, May 2005, Quebec City, Canada.

JA054599K